Coordination Chemistry Reviews, 105 (1990) 155–179
Elsevier Science Publishers B.V., Amsterdam

IRON BIOAVAILABILITY AND THE COORDINATION CHEMISTRY OF HYDROXAMIC ACIDS

ALVIN L. CRUMBLISS

Department of Chemistry, Duke University, Durham, NC 27706 (USA)

SUMMARY

The mechanism of iron bioavailability and the principles underlying siderophore affinity and specificity for iron are briefly reviewed. The kinetics and mechanism of iron dissociation from ferrioxamine B under conditions of low pH, or competing ligands, is discussed and compared with similar data for iron complexes with synthetic hydroxamic acids. Data are also presented for ferrioxamine B ligand exchange kinetics in the presence of surfactants. The mechanisms for the surfactant enhanced reactions are discussed and related to their possible relevance to iron dissociation from a hydroxamic acid siderophore complex at the cell surface.

INTRODUCTION

Iron is the second most abundant metal on the earth's surface, falling closely behind aluminum and in near equivalent concentration to calcium and sodium. Iron is an essential element for all living organisms and its key biological functions involve oxidation/reduction and interactions with O_2. The biological utility of an element is related to both its relative abundance and its accessibility (or bioavailability). Studies of microbial assimilation of this essential element have fascinated both chemists and biologists. The micro-organism must develop a mechanism to *selectively* make iron bioavailable. The selectivity of this mechanism is critical since numerous other metal ions are present in the environment which may not be essential or which may have a toxic effect on the organism. An example is aluminum, which is more abundant than iron, but which in many cases exerts a toxic effect on a living organism. The organism then must select iron over aluminum [1]. In addition to selectivity, another bioavailability consideration is the insolubility of the ferric ion in aqueous solution at physiological pH. This comes about because of the relatively large hydrolysis constants for Fe^{3+}_{aq} to form polymeric insoluble hydroxide containing compounds [2].

Coordination chemistry plays an important role in the assimilation of iron by micro-organisms. These microbes have developed polydentate chelating agents (siderophores) whose function is to selectively solubilize iron and transport it to the cell where it is then assimilated and incorporated into the biological machinery of the organism [3–8]. The mechanism of this process intimately involves fundamental concepts associated with coordination

0010-8545/90/$08.75

chemistry.

The synthesis and reactivity of coordination compounds is one of several areas of chemistry which Professor Basolo has had a major impact on. It is an honor and a pleasure to participate in this symposium honoring Fred Basolo on his seventieth birthday. Fred was conceiving and directing research programs in coordination chemistry which were relevant to important biochemical problems before bioinorganic chemistry was recognized as a buzz word or subspeciality of chemistry. It is under his guidance in his laboratory that I first learned the basic techniques and careful (and hopefully creative) thought processes of how to formulate and approach significant research problems in this important area of chemistry. I wish to thank him for that opportunity and his guidance.

SIDEROPHORE COMPLEXATION OF IRON

The processes involved in microbial iron assimilation are solubilization, transport to the cell, and deposition at an appropriate site within the cell [3-8]. The important chemical characteristics of the natural iron chelators which are relevant to these processes are affinity and selectivity for Fe^{3+}, and lability at a specific site (e.g., the cell wall or interior). This lability occurs either through ligand exchange, which often involves ternary complex intermediates, and/or a reduced oxidation state for iron (i.e., Fe^{2+}).

There are three components to consider in the design or evolution of a Fe^{3+}-specific (or any other metal) and high affinity chelating agent. These are: i) the type of Fe^{3+} binding group(s); ii) the number of binding groups in a particular molecule; and iii) the stereochemical arrangement of the binding groups [9]. Over a 100 siderophores have been isolated to date [4] and almost all contain either or both of the bidentate chelating groups:

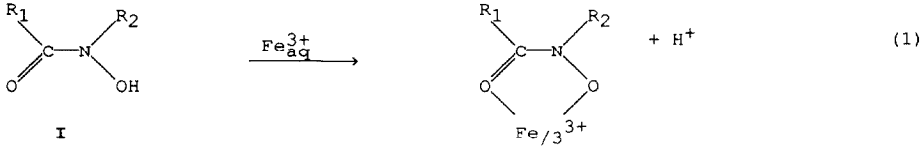

I (1)

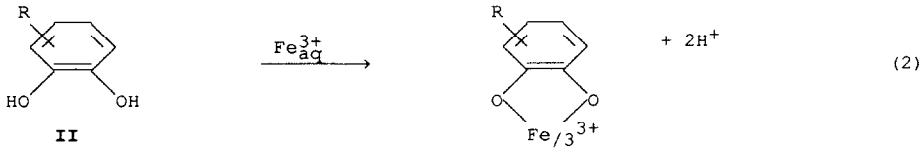

II (2)

hydroxamic acid (**I**) and catechol (**II**). For the most part, these ligands pro-

vide six coordinate chelate complexes with three stable five-membered ring chelate groups connected by a flexible backbone.

The high *stability* and Fe^{3+} *selectivity* considerations of the siderophores can best be viewed in light of the observation that Fe^{3+} is a hard Lewis acid with a high charge and high electronegativity. The presence of a negatively charged O atom donor in both the hydroxamate and catecholate Fe^{3+} chelating group undoubtedly plays a major role in producing thermodynamically stable complexes with Fe^{3+}. Iron(III) has a high affinity for the OH^- ion, the archetypal anionic oxygen donor ligand. This can be seen from the relatively large hydrolysis constant (log K_h = -2.56) for the $Fe(H_2O)_6^{3+}$ ion

$$Fe(H_2O)_6^{3+} \overset{K_h}{\rightleftharpoons} Fe(H_2O)_5OH^{2+} + H^+ \qquad (3)$$

[2]. A linear correlation between pK_h for a number of different metal ions and the product of metal ion electronegativity times charge ($\chi_M \cdot Z$) exists [1] which suggests that the high affinity that Fe^{3+} exhibits for OH^- is a result of the high charge and electronegativity of the ion.

Figure 1 is a plot of pM [7] values for various metal-ligand complexes versus the product of electronegativity times charge for a wide range of +2 and +3 metal ions. Good linear relationships exist for these data which demonstrate that metal ion affinity for a particular chelate increases with increasing metal ion electronegativity and/or charge. The plot further demonstrates that the high affinity of the catecholate and hydroxamate chelate groups for Fe^{3+} is a result of the Fe^{3+} ion being a strong, hard Lewis acid with a high $\chi_m Z$.

The selectivity of a ligand for specific metal ions is illustrated by the slopes of the lines in Figure 1. Catechol and the hydroxamic acids exhibit large slopes, with the trihydroxamate siderophore deferriferrioxamine B (**III**) exhibiting the largest slope of the chelators shown in Figure 1. The high

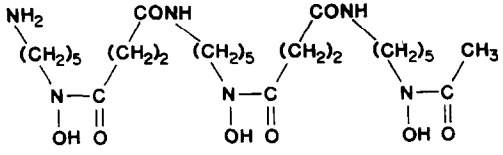

Deferriferrioxamine B (H_3DFB)

III

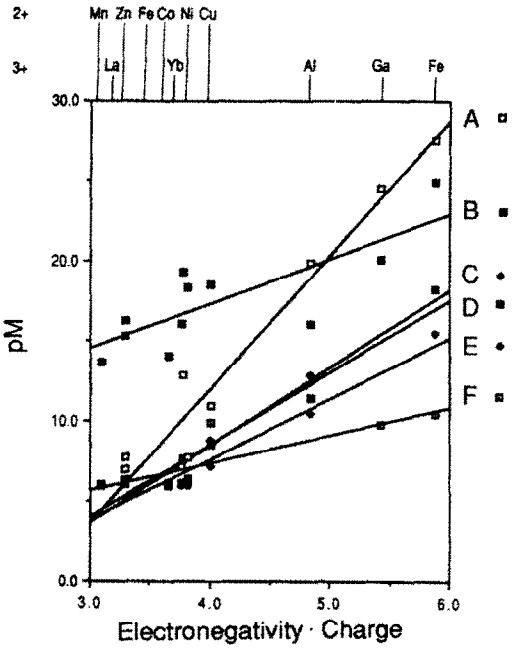

Fig. 1. Plot of pM values vs. electronegativity·charge ($\chi_M \cdot Z$) product at pH 7 for a range of 2+ and 3+ metal ions with A deferriferrioxamine B (8.3), B EDTA (2.8), C catechol (4.8), D acetohydroxamic acid (4.5), E salicyclic acid (3.8), and F glycine (1.7). Slopes of the plots are given in parentheses. Linear correlations are defined for more metal ion data points than are shown. Metal-ligand stability constant data obtained from Refs. [10-12] and electronegativity data from Ref. [13].

selectivity of the siderophores can be seen to result from the high electronegativity and charge of Fe^{3+}, and the sensitivity of the hydroxamic acid and catechol chelating groups to changes in either or both of these parameters. Most other biological or environmental metal ions tend to have a +2 charge (with the exception of the Al^{3+} ion) and lower electronegativity [1]. These and other relevant aspects of metal-ligand complex stability are discussed more completely in several recent reviews [1,4,7,9,11].

In addition to siderophore metal ion affinity and selectivity, a third aspect of the microbial iron assimilation process is removal of iron from its siderophore complex in order to deposit it at an appropriate cite on the cell surface or cell interior. Stated in a different way, the Fe^{3+}-selective chelator which forms a highly stable complex with iron must somehow increase its lability and release the bound iron on demand. This then becomes a mechanistic problem where a reaction pathway or pathways for iron dechela-

tion become available at a suitable time and location. Here the mechanistic literature of the coordination chemist becomes helpful in elucidating possible iron-siderophore dissociation pathways. These include: i) a pH decrease; ii) ternary complex formation with membrane bound or intracellular ligands, or inorganic ions such as Cl^-; iii) oxidation/reduction to form the more labile Fe^{2+} complex; iv) environmental effects such as the hydrophobicity/hydrophilicity of the medium; v) cell surface effects which may include charge and molecular recognition or receptor sites.

In this paper we feature the iron coordination chemistry of the hydroxamic acids, particularly of the siderophore deferriferrioxamine B (**III**), and some kinetic studies which relate to the general process of siderophore mediated iron bioavailability. The ferrioxamine B studies are intended to illustrate *in vitro* chemical mechanisms applicable to hydroxamate siderophore mediated iron bioavailability mechanisms in general, not the specifics of ferrioxamine B pathways *in vivo*.

FERRIOXAMINE B KINETIC STUDIES

Deferriferrioxamine B is a linear trihydroxamic acid siderophore whose structure is shown in **III**. The kinetics and mechanism of the formation and aquation of its iron complex, ferrioxamine B (**IV**), are probably the most

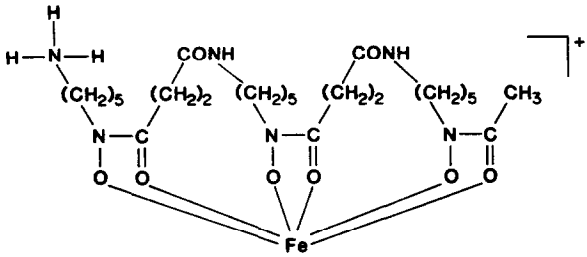

Ferrioxamine B ($Fe(HDFB)^+$)

IV

studied of the iron siderophore complexes [14-21]. This is likely due to the stability and ready availability of the ligand as a result of its use as a therapeutic agent in the treatment of individuals with acute [22] or chronic [23] iron poisoning and iron overload associated with β-thalassemia (Cooley's Anemia) [24,25]. Relevant ligand exchange reactions with ferrioxamine B have also been investigated [26,27].

The simple mono-hydroxamic acid, acetohydroxamic acid ($CH_3C(O)N(OH)H$), may be viewed as a model for the Fe^{3+} binding site in trihydroxamic acid

siderophores. The tris Fe^{3+} complex is readily formed in aqueous medium and

$$Fe^{3+}_{(aq)} + 3\ CH_3C(O)N(O)H^- \rightleftharpoons Fe(CH_3C(O)N(O)H)_3 \quad (4)$$

$\log \beta_3 = 28.29$ [28]; $\Delta H^0 = -5.9$ kcal/mole and $\Delta S^0 = 112$ eu [29-31]

$$Fe^{3+}_{(aq)} + HDFB^{2-} \rightleftharpoons FeHDFB^{+} \quad (5)$$

$\log \beta = 30.6$ [28]; $\Delta H^0 = -19.8$ kcal/mole and $\Delta S^0 = 71$ eu [30,32]

its stability is comparable with that of ferrioxamine B. However, the enthalpy and entropy parameters suggest there may be some subtle differences in the reasons for this similarity in Fe^{3+} binding affinity. The more positive entropy change for the tris acetohydroxamate complex may be due to the larger entropy of desolvation for three acetohydroxamate anions relative to the $HDFB^{2-}$ anion. The more exothermic enthalpy change for the complexation of Fe^{3+}_{aq} by $HDFB^{2-}$ may be a result of the larger inductive electron donor strength of the N-atom substituent in H_4DFB^+ ($-(CH_2)_5-$) than in acetohydroxamic acid (-H). Iron(III) stability constant measurements with C- and N-substituted synthetic hydroxamic acids show that a definite trend exists whereby stability increases with electron donor ability of both the C- and N-substituent, with the influence of the N-substituent being dominant [29,33]. This is consistent with an inductively stabilized N atom lone electron pair delocalized into the C-N bond, placing additional negative charge density on the carbonyl O atom (**V** and **VI**) as the dominant feature in determining changes in

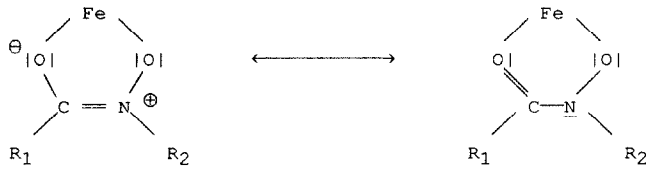

V **VI**

stability constants with changes in C- and N-substituent.

The metal-hydroxamic acid resonance picture represented in **V** and **VI** is supported by available structural data. X-ray crystal structures show that C-N and C-O bond distances in Fe^{3+} hydroxamate complexes are influenced by the N-substituent, with inductive electron releasing groups shortening the C-N and elongating the C-O bonds [34-44].

Acid dissociation

The dechelation kinetics of ferrioxamine B in strong acid is not of

direct biological relevance. However, an elucidation of the dechelation mechanism under experimental conditions where complete dechelation can occur (strong acid) provides a basis for understanding the stepwise dechelation process in neutral or weakly acid media. Furthermore, these data also enhance our understanding of biologically relevant ligand interchange processes and catalyzed iron release from many different siderophore structures. The most complete investigations of the stepwise dissociation of Fe^{3+} from ferrioxamine B in acidic medium in the absence of coordinating anions were performed by Monzyk and Crumbliss [14,15], and Wilkins, Pribanić, and co-workers [16]. These two studies are largely in agreement, although some significant differences are also evident. Both studies were carried out at acidic conditions to prevent complications from hydroxy complex formation and both utilized a sudden decrease in pH to drive the dechelation process. There is general agreement between both laboratories [14-16] that there are four kinetically detectable ferrioxamine B dechelation steps operable with rate constants which span five orders of magnitude (from 10^2 M^{-1} s^{-1} to 10^{-3} M^{-1} s^{-1}).

A comparison of the kinetics of dechelation of tris(acetohydroxamato)-iron(III), $Fe(CH_3C(O)N(O)H)_3$, and $FeHDFB^+$ in acid solution will serve as a model for the mechanism of linear trihydroxamic acid siderophore dissociation. A complete study of the equilibria, kinetics, and mechanism for tris(acetohydroxamato) iron(III) aquation in aqueous acid solution at conditions identical to the ferrioxamine B aquation studies was carried out by Pribanić, Wilkins and co-workers [45]. The acetohydroxamate ligand serves as a model for each hydroxamate group of ferrioxamine B.

The first step in the scheme is the dissociation and protonation of the first hydroxamate group of ferrioxamine B to form the tetracoordinate complex. An important feature of $FeHDFB^+$ is that dechelation is initiated at the protonated amine end of the molecule, based on analogy with aquation/formation kinetic studies of synthetic mono-hydroxamic acid complexes with Fe^{3+}, $Fe(R_1C(O)N(O)R_2)(H_2O)_4^{2+}$ [15,29,33,46]. A discrepancy between the two reports [15,16] concerns whether the protonation occurs before or after the rate limiting process in the production of the tetracoordinate intermediate,

$$Fe(HDFB)^+ + H^+ \underset{k_{-1}}{\overset{k_1}{\rightleftharpoons}} Fe(H_2DFB)(H_2O)_2^{2+} \qquad (6)$$

$$Fe(CH_3C(O)N(O)H)_3 + H^+ \underset{k_{-1}'}{\overset{k_1'}{\rightleftharpoons}} Fe(CH_3C(O)N(O)H)_2(H_2O)_2^+ + CH_3C(O)N(OH)H \qquad (7)$$

$Fe(H_2DFB)(H_2O)_2^{2+}$. Monzyk and Crumbliss [15] report an acid independent rate constant (290 s^{-1}) for the dechelation of $Fe(HDFB)^+$ to form the tetradentate

species $Fe(H_2DFB)(H_2O)_2^{2+}$. Wilkins, *et al.* report a value for k_1 = 380 M^{-1} s^{-1} [16] and $k_1 = 1.0 \times 10^5$ M^{-1} s^{-1} [45]. Apparently dissociation of a hydroxamate group from $Fe(CH_3C(O)N(O)H)_3$ is a kinetically more facile process than from $Fe(HDFB)^+$. This may reflect the influence of the hydrophobic connecting chain(s) in $Fe(HDFB)^+$ which hinder attack by the hydrated proton [16].

For ferrioxamine B an intermediate is formed between the tetradentate $Fe(H_2DFB)(H_2O)_2^{2+}$ and bidentate $Fe(H_3DFB)(H_2O)_4^{3+}$ structures. Although the structures of $Fe(H_2DFB)(H_2O)_2^{2+}$ and $Fe(H_3DFB)(H_2O)_4^{3+}$ [15,16] may be inferred from proton stoichiometries and spectral comparisons with synthetic mono-hydroxamate complexes of Fe^{3+} [29,45], the structure of the intermediate, $Fe(H_2DFB)(H_2O)_x^{2+*}$, formed in the proton independent step between the tetra- and bidentate forms of the dechelating ferrioxamine B complex is speculative.

Further dechelation to form the bidentate chelated ferrioxamine B from the half chelated intermediate and the corresponding acetohydroxamate/Fe^{3+} dissociation reaction may be represented as follows. Wilkins, *et al.* report

$$Fe(H_2DFB)(H_2O)_x^{2+*} + H^+ \underset{k_{-2}}{\overset{k_2}{\rightleftharpoons}} Fe(H_3DFB)(H_2O)_4^{3+} \tag{8}$$

$$Fe(CH_3C(O)N(O)H)_2(H_2O)_2^{+} + H^+ \underset{k'_{-2}}{\overset{k'_2}{\rightleftharpoons}} Fe(CH_3C(O)N(O)H)(H_2O)_4^{2+} + CH_3C(O)N(OH)H \tag{9}$$

a value for $k_2 = 2.3 \times 10^{-2}$ M^{-1} s^{-1} [16] and $k'_2 = 1.4 \times 10^3$ M^{-1} s^{-1} [45]. Monzyk and Crumbliss report a value for the corresponding process as $k_2 < 7.2 \times 10^{-2}$ M^{-1} s^{-1} [15]. The proton assisted dechelation of the second hydroxamate residue from ferrioxamine B is five orders of magnitude slower than dissociation of the second hydroxamate group from $Fe(CH_3C(O)N(O)H)_3$. Again the hydrophobicity and/or steric constraint of the siderophore backbone may be playing a role.

The slowest step in the overall ferrioxamine B dechelation process is the dissociation of the last hydroxamate group. This final step proceeds by parallel paths for both $Fe(H_3DFB)(H_2O)_4^{3+}$ and $Fe(CH_3C(O)N(O)H)(H_2O)_4^{2+}$ to

$$Fe(H_3DFB)(H_2O)_4^{3+} + H^+ \underset{k_{-3}}{\overset{k_3}{\rightleftharpoons}} Fe(H_2O)_6^{3+} + H_4DFB^+ \tag{10}$$

$$Fe(H_3DFB)(H_2O)_4^{3+} \underset{k_{-4}}{\overset{k_4}{\rightleftharpoons}} Fe(H_2O)_5OH^{2+} + H_4DFB^+ \tag{11}$$

$$Fe(CH_3C(O)N(O)H)(H_2O)_4^{2+} + H^+ \underset{k'_{-3}}{\overset{k'_3}{\rightleftharpoons}} Fe(H_2O)_6^{3+} + CH_3C(O)N(OH)H \tag{12}$$

$$Fe(CH_3C(O)N(O)H)(H_2O)_4^{2+} \underset{k'_{-4}}{\overset{k'_4}{\rightleftharpoons}} Fe(H_2O)_5OH^{2+} + CH_3C(O)N(OH)H \tag{13}$$

produce $Fe(H_2O)_6^{3+}$ and $Fe(H_2O)_5OH^{2+}$. Wilkins *et al.* report values of 5×10^{-4} M^{-1} s^{-1} and 9.3×10^{-4} s^{-1} for k_3 and k_4, respectively, which were obtained from equilibrium data and formation rate studies [16]. Monzyk and Crumbliss report corresponding values of 1.9×10^{-3} M^{-1} s^{-1} and 2.1×10^{-3} s^{-1} for k_3 and k_4 by studying the dissociation reaction directly [15], which is in reasonable agreement with Wilkins *et al.* results. The corresponding values for acetohydroxamic acid dissociation are 1.1×10^{-1} M^{-1} s^{-1} for k_3' and 7.9×10^{-2} s^{-1} for k_4' [29]. These data again show that dissociation of an acetohydroxamate group from Fe^{3+} is faster than dechelation of a hydroxamate moiety in ferrioxamine B, this time by two orders of magnitude.

The existence of parallel dissociation paths for the final step in ferrioxamine B aquation is a result of the strong tendency for the aquo ferric ion, $Fe(H_2O)_3^{3+}$, to hydrolyze [1]. The mechanism of dissociation of the hydroxamate group by initial cleavage of the Fe-O(N) bond, with synchronous protonation from solution or a *cis* coordinated water molecule, is based on kinetic investigations of Fe_{aq}^{3+} chelation and dissociation by a series of synthetic mono-hydroxamic acids $R_1C(O)N(OH)R_2$ [29,33,46]. Hydrolysis of partially chelated ferric ion is relatively unimportant in acidic medium, so the parallel acid independent dechelation step involving an intramolecular proton transfer from Fe^{3+} coordinated H_2O as shown in **VII** is only observed in the final step.

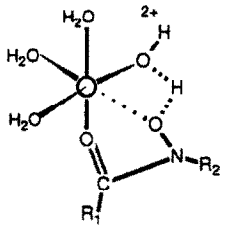

VII

The greater kinetic efficiency of the final hydroxamate group dissociation in the acetohydroxamic acid complex relative to ferrioxamine B may be in part due to the hydrophobic effect of the connecting backbone in the siderophore. However, the *acid independent* intramolecular H^+ transfer path is also two orders of magnitude greater for the acetohydroxamate system than for ferrioxamine B (eqns 11 and 13). This suggests that something other than connecting backbone hydrophobicity is likely to be operative.

The structure of the linear trihydroxamic acid deferriferrioxamine B (**III**) is such that the substituent on the N atom of each hydroxamate moiety

is an electron releasing alkyl group. Comparison of the kinetic parameters for the final hydroxamate dissociation step between ferrioxamine B and a synthetic mono-hydroxamate ($R_1C(O)N(OH)R_2$) may be more appropriate for the case where R_2 is an alkyl group rather than H, as is the case with acetohydroxamic acid. For example, rate constants for the acid dependent and acid independent dissociation of the mono-N-methylacetohydroxamate complex of Fe^{3+}, $Fe(CH_3C(O)N(O)CH_3)-(H_2O)_4^{2+}$, are 2.8×10^{-3} M^{-1} s^{-1} and 2.7×10^{-3} s^{-1}, respectively [29]. This is comparable to the k_3 and k_4 values reported for the final step of ferrioxamine B dechelation (reactions (10) and (11)) [15,16].

A linear correlation has been observed for the log of the rate constants associated with the acid dependent and acid independent parallel paths (e.g. eqns (12) and (13)) for the aquation of eighteen different mono-hydroxamato complexes $Fe(R_1C(O)N(O)R_2)(H_2O)_4^{2+}$ (including a thiohydroxamate), where R_1 and R_2 are different alkyl, aryl and H substituents [29,33,46]. This linear correlation with a slope of unity suggests that all of the aquation reactions proceed *via* the same mechanism and that the transition states for the two parallel paths differ by a H^+. Inspection of the data reveals that both the R_1 and R_2 substituents influence aquation rates *via* both paths, but that the dominant substituent is the one at the R_2 position on the N atom. When R_2 = H (independent of the R_1 substituent) the aquation rate constants are the largest. When R_2 = alkyl (independent of the R_1 substituent) the aquation rate constants are relatively smaller. The R_2 = aryl hydroxamic acids exhibit rate constants that are intermediate in range, independent of the R_1 substituent. The rate constants for the final stage of the ferrioxamine B aquation (k_3 and k_4 in eqns (10) and (11)) fall on the extreme low end of this line in the region for the synthetic hydroxamates where R_2 = alkyl [9,14]. Conformity to this linear relationship suggests that the final dechelation step of ferrioxamine B proceeds by the same mechanism as the dissociation of the synthetic mono-hydroxamate group from $Fe(R_1C(O)N(O)R_2)-(H_2O)_4^{2+}$. Additional evidence for this mechanistic similarity comes from the activation parameters ($\Delta H^{\ddagger}$, $\Delta S^{\ddagger}$) for the forward and reverse parallel path process in the final ferrioxamine B dechelation step (eqns (10) and (11)) [30], which follow the same linear isokinetic $\Delta H^{\ddagger}$-$\Delta S^{\ddagger}$ relationship defined by eighteen synthetic hydroxamic acids [29,33,46].

The minimization of the acid dependent and acid independent aquation rate constants for the hydroxamic acids with R_2 = alkyl has been discussed [29,33,46] in terms of the inductive stabilization of the formal positive charge on N resulting from the delocalization of the N atom lone electron pair into the C-N bond. This places additional electron density on the car-

bonyl O atom as shown in resonance form V. Since the second and rate limiting bond cleavage for each hydroxamate group is Fe–(O)C, placing additional electron density on the carbonyl O atom retards the hydroxamate dissociation rate.

Our analysis suggests that the small rate constant for the final dissociation step of ferrioxamine B *via* the acid dependent and acid independent paths may be due to the electronic influence of the N-alkyl substituent. This also suggests that electronic factors may at least be partially responsible (in addition to possible hydrophobic and steric effects) for the smaller rate constants in the earlier stages of ferrioxamine B dechelation relative to the acetohydroxamic acid complex.

Ternary complex formation

Although ferrioxamine B dechelation in strongly acidic medium as described above is not directly comparable to siderophore mediated iron transport at biological conditions, an understanding of the process provides some insight into possible *in vivo* catalytic pathways for a whole range of siderophores. As dechelation of ferrioxamine B occurs, vacant coordination sites on Fe^{3+} become available for competing ligands and metal free binding sites on the deferriferrioxamine B become available for chelation to other metal ions. The latter case has been illustrated by Pribanić and co-workers [19,30,47-49] and Pribanić, Wilkins and co-workers [16] who have observed the production of diferrioxamine B, $Fe_2(HDFB)^{4+}$, in the reaction of Fe^{3+}_{aq} and deferriferrioxamine B (H_4DFB^+), and in the dechelation of ferrioxamine B in the presence of excess Fe^{3+}_{aq}. Such a species is not likely to be important in terms of siderophore mediated iron bioavailability, but it does suggest the possibility for excess metal ions of some sort taking the place of a H^+ ion in preventing ring re-closure during the dechelation process for ferrioxamine B or other hydroxamate siderophores [9].

A similar example may be seen in the citrate promoted reductive removal of iron from the hydroxamate siderophores rhodotorulic acid, ferrichrome, ferrioxamine B, triacetyl fusarinine C and ferrichrome A, which occurs only in the presence of Ga^{3+} [50]. Apparently Ga^{3+} plays the role of H^+ in preventing ring closure of the dissociating siderophore and enhances the accessibility of the Fe^{3+} to the citrate reducing agent.

Inorganic ions such as Cl^- can enhance ferrioxamine B dissociation kinetics, presumably by ternary complex formation. This may be seen by comparing ferrioxamine B chelation/dechelation kinetic data obtained in aqueous media containing $NaClO_4$ (2.0 M) and NaCl (1.0 M) background electrolytes [16,20]. The last step of the ferrioxamine B dechelation process is repre-

sented in eqns (10) and (11). The rate acceleration for each of the microscopic rate constants on changing the reaction medium from ClO_4^- to Cl^- is as follows (the number in parentheses represents the ratio of k_n in Cl^- medium to k_n in ClO_4^- medium) [16,20]: k_3 (1.3×10^3); k_{-3} (1.4×10^2); k_4 (1.7×10^1); k_{-4} (1.1). The observed rate constant increase is too large to be ascribed to a medium effect and clearly the biggest effect is in the non OH^- ligand path. Presumably Cl^- enters the coordination shell of Fe^{3+} and labilizes the dissociating donor atoms, which are either the hydroxamate group in the dechelation step or coordinated H_2O in the chelation step. This is similar to the labilizing effect of OH^- and probably explains why Cl^- has a lesser effect on the k_4/k_{-4} path (eqn (11)). Chloride ion has also been shown to have a similar labilizing effect on mono-(acetohydroxamato) and (betaine hydroxamato)iron(III) complex systems [47].

Kinetic results obtained in the presence of chloride ion illustrate the labilizing influence that small molecules or ions (ligands) may have in siderophore ligand exchange reactions. The kinetics and mechanism of the ferrioxamine B/EDTA exchange reaction (14) have been investigated [26,27]. The

$$Fe(HDFB)^+ + H_xEDTA^{(4-x)-} \rightleftharpoons FeEDTA^- + H_4DFB^+ \qquad (14)$$

addition of any one of several synthetic mono-hydroxamic acids ($CH_3C(O)N(OH)H$, $C_6H_5C(O)N(OH)H$, $CH_3C(O)N(OH)CH_3$) was found to catalyze the exchange reaction [27]. A detailed kinetic study which included spectrophotometric characterization of reactive intermediates was carried out at pH 5.4. The mechanism for the mono-hydroxamate catalyzed process involves four parallel paths, three of which include ternary complex formation to produce $Fe(H_2DFB)A^+$, $Fe(H_3DFB)A_2^+$ and FeA_3 (A = mono-hydroxamate anion) which lead to $FeEDTA^-$ product formation. Different stabilities of the various ternary complexes are reported which are consistent with the expected influence of the C and N substituents in the mono-hydroxamic acid catalyst. Catalysis presumably occurs as a result of the labilizing effect of the mono-hydroxamate in the inner coordination shell, which also prevents ferrioxamine B ring closure. Furthermore, the entering mono-hydroxamic acid may provide a proton to the dissociating ferrioxamine B *via* a H^+ transfer within the inner coordination shell, which prevents deferriferrioxamine B ring closure.

LIGAND EXCHANGE KINETICS IN THE PRESENCE OF SURFACTANTS

The previous discussion has illustrated the pH sensitivity of Fe^{3+} dissociation from ferrioxamine B and the effect of Cl^- and low molecular weight chelators (e.g. mono-hydroxamic acids) on the enhancement of Fe^{3+} dissocia-

tion. While a redox process may be involved in *in vivo* iron release from ferrioxamine B and sudden large pH drops may not provide a particularly viable biological mechanism for Fe^{3+} deposition, ternary complex formation involving common environmental ions such as Cl^- or low molecular weight chelators is a reasonable pathway for Fe^{3+} deposition from some siderophore carriers at the cell surface or interior.

As another consideration we wish to devise *in vitro* experiments which may probe the influence that the aqueous/cell interface may have on enhancing Fe^{3+} dissociation from a siderophore complex. In these experiments we employ various cationic, anionic and neutral surfactants to produce micelles. These micelles serve as models for the aqueous/hydrophobic barrier associated with a cell surface [51,52]. The experimental approach is to investigate the kinetics and mechanism of Fe^{3+} exchange between a hydrophilic chelator in an aqueous environment (siderophore or model siderophore) and a hydrophobic chelator associated within a micelle (Scheme A). These data will then be

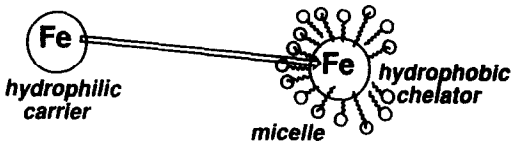

SCHEME A

compared with similar data obtained in the absence of surfactants. We are interested in looking for possible surface effects (e.g. charge), ternary complex formation, and any role orientation or molecular recognition might play in enhancing ligand exchange rates. Again, the prototype siderophore used in these experiments is ferrioxamine B, not because the objective is to probe the *in vivo* iron bioavailability mechanism for ferrioxamine B specifically, but rather to use ferrioxamine B as a prototype linear hydroxamate siderophore for which we have detailed kinetic and mechanistic data on uncatalyzed Fe^{3+} dechelation to aid in our interpretation of any catalytic mechanisms.

The hydrophobicity of the hydroxamic acids can be controlled by varying the substituent on the C or N atom. For example, changing the C substituent from $-CH_3$ (acetohydroxamic acid, hydrophilic), to $-C_6H_5$ (benzohydroxamic acid, hydrophobic), to a seven-carbon chain (octanohydroxamic acid, hydrophobic) provides for a wide range of hydrophobic control. Octanohydroxamic acid is an amphiphilic molecule that can form co-micelles with other surfactants [53,54].

In a solution containing micelles, acetohydroxamic acid is in the aqueous phase while benzo- and octano-hydroxamic acids reside in the micelle pseudo-phase [54]. This variation allows us to investigate Fe^{3+}/ligand exchange reactions in the presence of micelles whereby Fe^{3+} is transferred from a hydrophilic carrier to a tris(hydroxamate) binding site which is located in aqueous medium or within the micelle pseudo-phase. The uv-visible absorption spectrum of tris(hydroxamato)iron(III) complexes is sensitive to solvent environment. This can be used to establish that $Fe(RC(O)N(O)H)_3$ occurs in the aqueous phase when R = CH_3 (acetohydroxamic acid) and in the micelle pseudo-phase when R = C_6H_5 or C_7H_{15} (benzo or octanohydroxamic acid) [54].

In our investigations we have used cationic (CTAB), anionic (SDS) and uncharged (Triton X) surfactants to produce micelle containing solutions. Appropriate control experiments were performed to ensure that any surfactant influence on Fe^{3+}-ligand exchange kinetics was not due to specific ion or ionic strength effects.

Iron EDTA/hdroxamic acid ligand exchange

We have investigated the influence of surfactants on the Fe^{3+}-ligand exchange reaction (15), whereby Fe^{3+} is exchanged from the hydrophilic

$$FeEDTA^- + 3\ RC(O)N(OH)H \xrightarrow{S} Fe(RC(O)N(O)H)_3 + H_xEDTA^{x-4} \qquad (15)$$

R = CH_3, C_6H_5, C_7H_{15}; S = CTAB, SDS, Triton X

carrier, EDTA, to a tris-hydroxamate complex [55]. The rate of the reaction of $FeEDTA^-$ with the hydrophilic acetohydroxamic acid is not influenced by charged or uncharged surfactants. The reaction rate of $FeEDTA^-$ with the hydrophobic chelators benzo- or octano-hydroxamic acid is not influenced by neutral or negatively charged surfactants, but is influenced by CTAB, a positively charged surfactant. Figure 2 illustrates the increase in rate constant observed for reaction (15) in the presence of CTAB concentrations above the critical micelle concentration [55].

The parallel path reaction shown in Scheme B involving Fe^{3+}-ligand exchange in aqueous medium and at the micelle pseudo-phase surface is consistent with data obtained at various H^+ and hydroxamic acid concentrations for reaction (15) in the presence of CTAB. Table 1 lists the micelle binding constants, K_m, and microscopic rate constants associated with the aqueous phase, k_{aq}, and the micelle pseudo-phase, k_m, which were calculated using the Berezin model [56]. k_{aq} values were obtained from experiments using acetohydroxamic acid where k_m and k_m' are zero. The partially hydrolyzed $Fe(OH)(EDTA)^{2-}$ was assumed to be only associated with the micelle surface

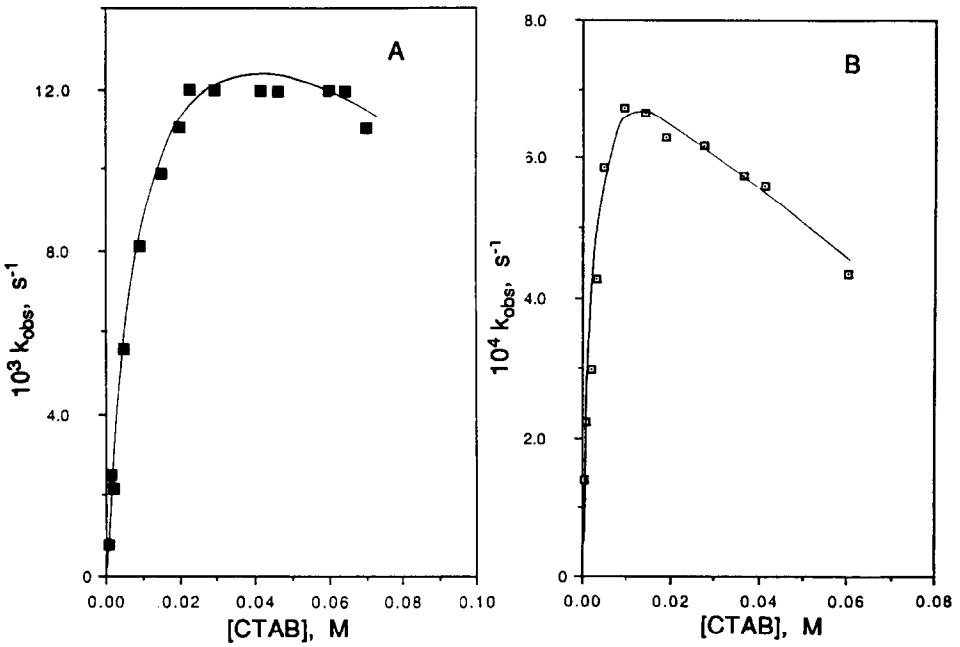

Fig. 2. Pseudo-first-order rate constant for reaction (15) plotted as a function of CTAB concentration for A benzohydroxamic acid ($PhC(O)N(OH)H$) and B octanohydroxamic acid ($CH_3(CH_2)_6C(O)N(OH)H$). Conditions: pH = 7.0 (0.05 M Tris); 25°C; [$FeEDTA^-$] = 2.0×10^{-4} M; A [$PhC(O)N(OH)H$] = 0.10 M; B [$CH_3(CH_2)_6C(O)N(OH)H$] = 0.006 M. CTAB cmc in 0.05 M Tris buffer; pH 7.0 at 25°C is 5.1×10^{-5} M. CTAB/octanohydroxamic acid co-micellar cmc at 6.0×10^{-3} M $CH_3(CH_2)_6C(O)N(OH)H$, in 0.05 M Tris buffer, pH 7.0 at 25°C is 4.0×10^{-5} M. All data from Ref. [55].

$$FeEDTA^-_{aq} + HA_{aq} \xrightarrow{k_{aq}} Fe(HEDTA)(A)^-_{aq} \xrightarrow{2HA} FeA3_m + H_2EDTA^{2-}_{aq} \quad (16)$$

$$K_m^{Fe} \uparrow\downarrow \qquad K_m^{HA} \uparrow\downarrow$$

$$FeEDTA^-_m + HA_m \xrightarrow{k_m} Fe(HEDTA)(A)^-_m \xrightarrow{2HA} FeA3_m + H_2EDTA^{2-}_{aq} \quad (17)$$

$$K_{OH} \uparrow\downarrow H^+$$

$$Fe(OH)(EDTA)^{2-}_m + HA_m \xrightarrow{k_m'} Fe(EDTA)(A)^-_m \xrightarrow{2HA} FeA3_m + H_2EDTA^{2-}_{aq} \quad (18)$$

SCHEME B. HA = $PhC(O)N(OH)H$, $CH_3(CH_2)_6C(O)N(OH)H$, *aq* designates aqueous phase, and and *m* designates micelle pseudo-phase.

due to its high negative charge [57]. Evidence for the validity of the Berezin model in analyzing these data may be seen in the relatively constant

value obtained for $FeEDTA^-$ aqueous/micelle binding constant, K_m^{Fe}, and the increase in the corresponding hydroxamic acid binding constant, K_m^{HA}, on going from benzohydroxamic acid to the more hydrophobic octanohydroxamic acid (Table 1).

Comparison of k_m and k_{aq} values in Table 1 indicates that the cationic

TABLE 1 [55]

Microscopic constants associated with Scheme B in the presence of CTAB.

Parameter	Hydroxamic Acid	
	$C_6H_5C(O)N(OH)H$	$C_7H_{15}C(O)N(OH)H$
K_m^{Fe}/M^{-1}	20	30
K_m^{HA}/M^{-1}	30	154
K_{OH}/M^a	2.6×10^{-8}	2.6×10^{-8}
$k_{aq}/M^{-1}\ s^{-1}{}^b$	3.5×10^{-3}	3.5×10^{-3}
$k_m/M^{-1}\ s^{-1}$	9.1×10^{-4}	6.9×10^{-5}
$k_m'/M^{-1}\ s^{-1}$	2.9×10^{-2}	1.1×10^{-2}

[a] Obtained from Ref. [26] in aqueous medium.
[b] Value listed is for $CH_3C(O)N(OH)H$ where k_m and $k_m' = 0$.

CTAB surfactant has little influence on the microscopic rate constant for Fe^{3+}/ligand exchange at the micelle surface. Rather the rate enhancement observed in the presence of CTAB (see Figure 2 for example) is due to a preconcentration or proximity effect as suggested by the K_m^{Fe} and K_m^{HA} values. Apparently the charged micelle surface enhances the concentration of the $FeEDTA^-$/hydroxamic acid encounter complex, but does not influence the reactivity of the $FeEDTA^-$ coordination shell. The smaller k_m value for octanohydroxamic acid suggests a deeper partitioning of this more hydrophobic hydroxamic acid within the micellar region. The enhanced reactivity of the partially hydrolyzed EDTA complex, $Fe(OH)(EDTA)^{2-}$, at the micelle surface (k_m'/k_m) is consistent with the known labilizing influence of OH^- in the inner coordination shell.

The mechanistic picture developed for reaction (15) in the presence of surfactants is one in which the ligand exchange reaction is proceeding in parallel paths in aqueous medium and on the micelle surface. A rate enhancement is observed when the micelle surface serves to bring the reacting partners together in close proximity. Such is the case when the micelle surface is positively charged (CTAB) and the hydroxamic acid is preferentially partitioned into the micelle pseudo-phase (benzo- and octanohydroxamic acid).

Ferrioxamine B/hydroxamic acid exchange

The Fe^{3+} ligand exchange reaction (19) between ferrioxamine B and benzo-

$$FeHDFB^{+}_{aq} + 3\ PhC(O)N(OH)H_m \xrightarrow{S} Fe(PhC(O)N(O)H)_{3m} + H_4DFB^{+}_{aq} \qquad (19)$$

S = CTAB, SDS, Triton X

hydroxamic acid has been investigated in the presence of various surfactants over a wide range of H^+ and PhC(O)N(OH)H concentrations [58]. The negatively charged surfactant SDS has been found to accelerate the rate of this exchange reaction as is illustrated in Figure 3. Positive and neutral surfactants

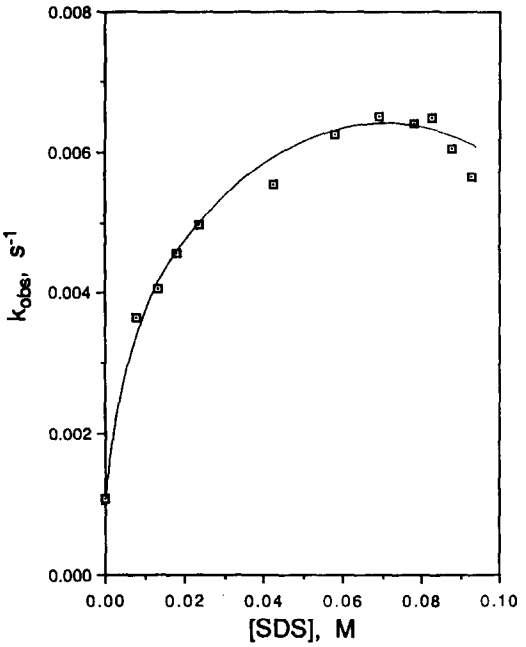

Fig. 3. Pseudo-first-order rate constant for reaction (19) plotted as a function of SDS concentration. Conditions: pH = 7.1 (0.05 M Tris); 25.0°C; $[FeHDFB^+]$ = 7.5 x 10^{-5} M; [PhC(O)N(OH)H] = 0.1 M, SDS cmc = 2.0 x 10^{-3} M [59]. Data from Refs. [54,58].

have no influence on reaction (19). The pseudo-first-order rate constant for reaction (19) at a given SDS concentration exhibits a non-linear dependence on [Ph(C(O)N(OH)H], as well as a strong pH dependence as illustrated in Figure 4.

The three step mechanism shown in Scheme C is consistent with the kinetic data. The mechanism involves ferrioxamine B hydroxamate chelate ring opening (eqn (20)) and benzo-hydroxamic acid ternary complex formation on the micelle surface (eqn (21)), followed by rapid formation of the tris(benzohydroxamic

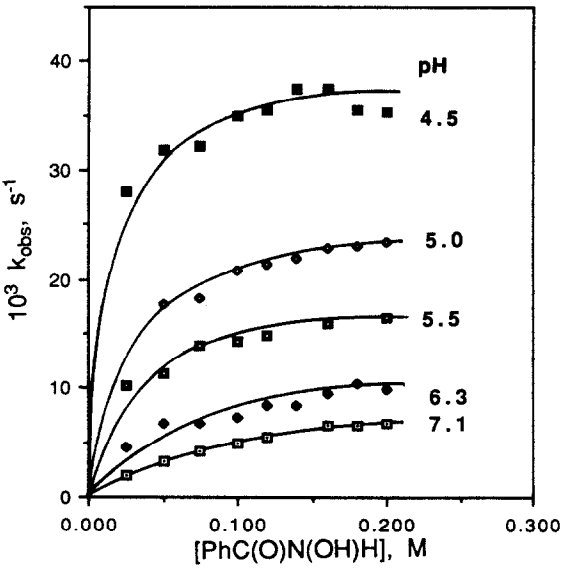

Fig. 4. Pseudo-first-order rate constant for reaction (19) plotted as a function of PhC(O)N(OH)H concentration at various pH values. Conditions: 25.0°C; [SDS] = 0.04 M; [$FeHDFB^+$] = 7.5 x 10^{-5} M. Data from Ref. [58].

$$FeHDFB^+ + H^+ \underset{k_{-1}}{\overset{k_1}{\rightleftharpoons}} Fe(H_2DFB)(H_2O)_2^{2+} \quad (20)$$
aqueous

$$Fe(H_2DFB)(H_2O)_2^{2+} + PhC(O)N(OH)H \xrightarrow{k_2} Fe(H_2DFB)(PhC(O)N(O)H)^+ + H^+ \quad (21)$$

$$Fe(H_2DFB)(PhC(O)N(O)H)^+ + 2\ PhC(O)N(OH)H \xrightarrow{fast} \underset{micelle}{Fe(PhC(O)N(O)H)_3} + \underset{aqueous}{H_4DFB^+} \quad (22)$$

SCHEME C

acid)iron(III) complex in the micelle interior (eqn (22)). Microscopic rate constants may be obtained from kinetic data using the following algebraic

$$k_{OBS} = \frac{a[BHA]}{b + [BHA]} \quad (23)$$

expression where $a = [H^+]k_1$ and $b = k_{-1}/k_2$. Assuming $k_1/k_{-1} = 10\ M^{-1}$ as established independently in aqueous solution [15,28], microscopic rate constants obtained from kinetic data at variable PhC(O)N(OH)H and H^+ concentrations and a fixed SDS concentration are $k_1 = 1.1 \times 10^5\ M^{-1}\ s^{-1}$ and $k_2 = 8.2 \times 10^4\ M^{-1}\ s^{-1}$. These microscopic rate constants are 3 orders of magnitude greater than values obtained for H^+ driven ferrioxamine B aquation or ligand

exchange reactions in the absence of surfactant micelles [15,16,26]. Apparently the micelle surface exhibits a significant influence on the dynamics of this ligand exchange reaction.

An important consideration in comparing an anionic surfactant system with aqueous data is the effect of the anionic micelle surface. There is an electrostatic attraction between the negatively charged surface and H^+ ions, which effectively decreases the pH at the surface [60,61]. This may be quantified using eqn (24) [60] where $[H^+]_b$ and $[H^+]_s$ are the H^+ concentrations in

$$[H^+]_s = [H^+]_b \exp(-eY/kT) \qquad (24)$$

the bulk and micelle surface, respectively, e the electronic charge, Y the surface potential (-120 mV [62] for SDS), k the Boltzmann constant and T the temperature. This equation predicts a 100 fold increase in H^+ concentration at the SDS micelle surface over that found in the bulk. If the ligand exchange reaction occurs at the SDS micelle surface, then given the pH sensitivity of the ferrioxamine B dechelation process it is reasonable that SDS surfactant molecules at concentrations above the cmc will enhance the ligand exchange reaction (19).

Equation (23) may be used to calculate an effective "kinetic" $[H^+]$ on the surface of the SDS micelle by inserting microscopic rate constants for the steps represented in Scheme C that are derived from H^+ driven ferrioxamine B dechelation, or ferrioxamine B ligand exchange kinetics, in the absence of surfactants [15,16,26,58]. This assumes that the SDS micelle does not influence the microscopic rate constants in Scheme C, only the surface $[H^+]$. For example, a surface $[H^+] = 3.8 \times 10^{-5}$ M was calculated in this way using data in which the measured bulk aqueous $[H^+] = 7.9 \times 10^{-8}$ M. This pH drop is consistent with the calculation using eqn (24).

The mechanistic picture that emerges from this study [58] is that in the presence of negatively charged head group surfactants ferrioxamine B exchanges Fe^{3+} with micelle encapsulated benzohydroxamic acid on the surface of the micelle at significantly faster rates than in bulk aqueous solution due to the higher H^+ concentration on the micelle surface. The reaction proceeds through ternary complex formation on the micelle surface, with reactivity similar to that observed in bulk solution once the difference in surface H^+ concentration is accounted for. The influence of the negative SDS head group in bringing the positively charged $FeHDFB^+$ in close proximity to the benzohydroxamic acid undoubtedly also plays a role.

Ferrioxamine B/hydroxamic acid exchange in the presence of a crown ether

Receptor sites on the cell surface may appropriately orient an Fe^{3+} siderophore complex or increase its reactivity with respect to ligand exchange. Siderophore molecular recognition via coordination shell or ligand backbone geometry has been investigated in other laboratories [63]. We are interested in modeling the possibility of siderophore side chain recognition being involved in enhancing Fe^{3+} ligand exchange lability. We are also investigating ways in which a modified micelle surface may influence the dynamics of Fe^{3+}-ligand exchange reactions which occur on the surface.

In an attempt to model such a system we have studied the kinetics of ferrioxamine B/benzohydroxamic acid exchange in the presence of surfactants, with the additional feature of adding a hydrophobic crown ether to the reaction mixture, *cis*-dicyclohexyl-18-crown-6 (DC-18-C-6) [64]. This particular crown ether was selected for two reasons: it is hydrophobic and therefore is associated with the micelle and it has a cavity size appropriate for complexing primary ammonium ions [65].

DC-18-C-6 can readily complex the protonated amine side chain of aqueous ferrioxamine B and extract the iron complex into chloroform solution. Ferrioxamine B is not soluble in $CHCl_3$ and the extraction process illustrated in reaction (25) with $K_{eq} = 5\ M^{-1}$ [64] is indirect evidence for DC-18-C-6 complexation of the protonated amine side chain of ferrioxamine B. The uv-

$$FeHDFB_{(aq)}^{+} + DC\text{-}18\text{-}C\text{-}6_{(CHCl_3)} \underset{}{\overset{K\ =\ 5\ M^{-1}}{\rightleftharpoons}} FeHDFB^{+}\cdot DC\text{-}18\text{-}C\text{-}6_{(CHCl_3)} \qquad (25)$$

visible spectrum of $FeHDFB^{+}\cdot$DC-18-C-6 in $CHCl_3$ is similar to that observed for $FeHDFB^{+}$ in water. The K_{eq} value obtained for reaction (25) is in the range expected for protonated primary amine complexation by a cyclic polyether with the cavity size of an 18-crown-6 ring [66].

Figure 5 illustrates the influence of DC-18-C-6 on the pseudo-first-order rate constant, k_{obs}, for the ligand exchange reaction (26) in the presence of

$$FeHDFB_{aq}^{+} + 3\ PhC(O)N(OH)H_m \xrightarrow[S]{\text{DC-18-C-6}} Fe(PhC(O)N(O)H)_{3m} + H_4DFB_{aq}^{+} \qquad (26)$$

S = SDS, CTAB, Triton X

micelles formed by anionic (SDS), cationic (CTAB) and uncharged (Triton X) surfactants. The ligand exchange process is sensitive to increasing DC-18-C-6 concentrations and whether this results in an increase or decrease in rate depends on the head group charge on the surfactant. The k_{obs} for reaction (26) decreases with increasing DC-18-C-6 in SDS (negative head group) and increases with Triton X (uncharged head group) and CTAB (positive head group).

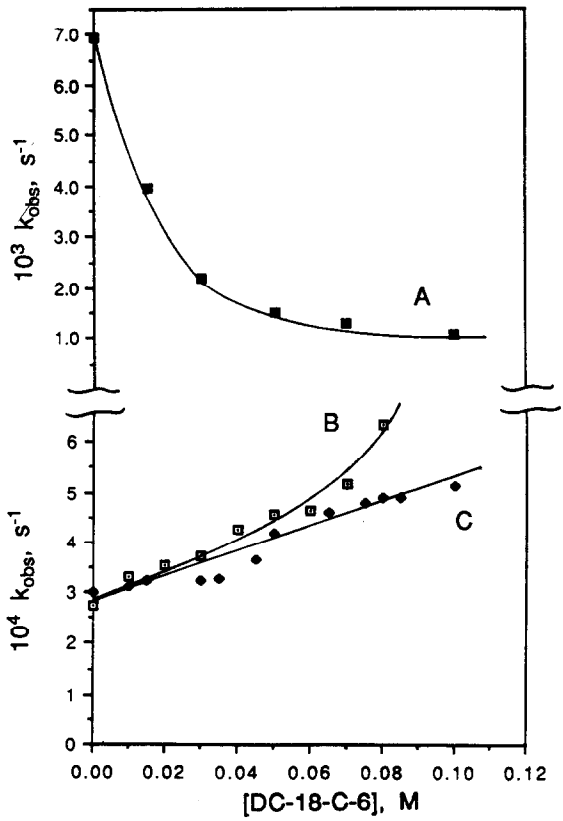

Fig. 5. Pseudo-first-order rate constant for reaction (26) in the presence of A SDS, B Triton X and C CTAB surfactants plotted as a function of dicyclohexyl-18-crown-6 concentration. Conditions: pH = 7.1; 25°C; [PhC(O)N(OH)H] = 0.10 M; [$FeHDFB^+$] = 7.5 x 10^{-5} M; [SDS] = 0.10 M; [Triton X] = 0.08 M; [CTAB] = 0.08 M. Data from Ref. [64].

Results presented in Figure 5 suggest that micelle bound DC-18-C-6 complexes the protonated amine arm of ferrioxamine B at the micelle surface, followed by Fe^{3+} exchange to form the tris(benzohydroxamato)iron(III) complex within the micelle pseudo-phase. Recall that Triton X and CTAB do not influence this Fe^{3+} ligand exchange reaction in the absence of crown ether (see above), presumably because there is no pH drop at the surface and no electrostatic attraction between the cationic $FeHDFB^+$ and CTAB or Triton X. Addition of DC-18-C-6 to Triton X or CTAB provides a pathway for $FeHDFB^+$ association with the micelle surface via complexation of the $-(CH_2)_5-NH_3^+$ side chain. This complexation at the micelle surface then enhances the ligand exchange process to form $Fe(PhC(O)N(O)H)_3$ within the micelle, either due to a proximity effect

or a labilization of $FeHDFB^+$ dissociation. In the presence of SDS, complexation of the $-(CH_2)_5NH_3^+$ side chain evidently prevents a kinetically significant electrostatic interaction between $-(CH_2)_5NH_3^+$ and the negatively charged head group, thus retarding the rate.

The model proposed is illustrated in Figure 6, in which DC-18-C-6, while

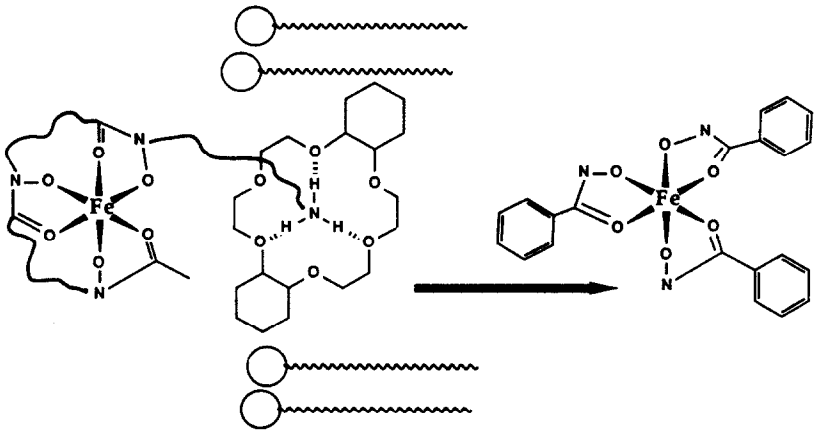

Fig. 6. Schematic representation of dicyclohexyl-18-crown-6 complexation of the $-(CH_2)_5-NH_3^+$ side chain of ferrioxamine B and subsequent ligand exchange to form $Fe(PhC(O)N(O)H)_3$ within the micelle.

associated with the surfactant micelle, "recognizes" ferrioxamine B by complexing the $-(CH_2)_5NH_3^+$ side chain. Additional supporting evidence for the model comes from similar experiments using the more hydrophilic crown ether of equivalent cavity size 1,4,7,10,13,16-hexaoxacyclooctadecane (18-C-6) [64]. In this case the crown ether is distributed in the aqueous phase and not largely confined to the micelle. The pseudo-first-order rate constant for Fe^{3+} ligand exchange in the presence of SDS surfactant (reaction (26)) decreases as in the case of DC-18-C-6. This is consistent with the aqueous crown complexing the protonated amine side chain of ferrioxamine B and decreasing the electrostatic attraction between cationic $FeHDFB^+$ and the SDS micelle surface. In the presence of Triton X and CTAB, 18-C-6 has no influence on the observed psuedo-first-order rate constant for reaction (26), consistent with there being no crown ether "molecular recognition" of the $-(CH_2)_5NH_3^+$ side chain of ferrioxamine B at the micelle surface.

CONCLUSIONS

Kinetic data obtained under various conditions for Fe^{3+} dissociation from ferrioxamine B have been presented as a model for non-reductive iron release from a hydroxamate siderophore. These data have been discussed within the

context of similar kinetic data for synthetic hydroxamic acid complexes of iron(III). Apparently the connecting chains between the hydroxamate groups in ferrioxamine B exert a rate retarding electronic influence on the dechelation kinetics, as well as steric and perhaps hydrophobic influences.

The question of possible non-reductive pathways for iron release from its high affinity siderophore carrier at the appropriate time and place is posed. High acidity, and competing ligands resulting in ternary complex formation, enhance the dissociation rates of Fe^{3+} from ferrioxamine B. The presence of certain surfactants are also found to enhance Fe^{3+} exchange rates from ferrioxamine B to a micelle bound synthetic hydroxamic acid chelator. The mechanism for this rate enhancement by surfactants includes ferrioxamine B ring opening at the micelle surface, where in the case of SDS a region of low pH exists. Rapid ternary complex formation occurs due to the micelle induced close proximity of ferrioxamine B and the micelle bound exchanging ligand. A micelle bound crown ether was found to further enhance this exchange process by encapsulating the protonated amine side chain of ferrioxamine B. These results may have relevance to *in vivo* iron dissociation from a hydroxamate siderophore where orientation, molecular recognition, and/or a localized pH decrease may serve to enhance the lability of the siderophore complexed iron at the cell surface.

Acknowledgements

The donors of the Petroleum Research Fund, administered by the American Chemical Society, are acknowledged for their support of our research in this area. The author thanks his co-workers whose names appear in the references, particularly P.L. Choo and S.W. Harman for use of their results prior to publication, and Professor D. van der Helm for a preprint of his manuscript.

REFERENCES

1 A.L. Crumbliss and J.M. Garrison, *Comments Inorg. Chem.*, 8 (1988) 1.
2 J. Kragten, *Atlas of Metal-Ligand Equilibria in Aqueous Solution*, Halstead Press, N.Y., 1978.
3 G. Winkelmann (Ed.), Handbook of Microbial Chelates, CRC Press, Boca Raton, Fla., in press.
4 B.F. Matzanke, G. Müller-Matzanke, and K.N. Raymond, in T.M. Loehr (Ed.), *Physical Bioinorganic Chemistry Series: Iron Carriers and Iron Proteins*, VCH Publ. Co., N.Y., 1989, chap. 1.
5 G. Winkelmann, D. van der Helm, and J.B. Neilands (Eds.), *Iron Transport in Microbes, Plants and Animals*, VCH Publ. Co., Weinheim, 1987.
6 J.B. Neilands, *Ann. Rev. Plant Phys.*, 37 (1986) 187.
7 K.N. Raymond, G. Müller, and B.F. Matzanke, in F.L. Boscheke (Ed.), *Topics in Current Chemistry*, Vol. 123, Springer-Verlag, N.Y., 1984, p. 49.
8 A. Chimiak (Ed.), *Siderophores from Microorganisms and Plants, Structure and Bonding*, Volume 58, Springer-Verlag, N.Y., 1984.

9 A.L. Crumbliss, in G. Winkelmann (Ed.), *Handbook of Microbial Chelates*, CRC Press, Boca Raton, Fla., in press.
10 A.E. Martell and R.M. Smith (Eds.), *Critical Stability Constants*, Vols. 1, 2, 3, 4, 5, and 6, Plenum Press, N.Y., 1974, 1975, 1977, 1976, 1982, and 1989.
11 R.D. Hancock and A.E. Martell, *Chem. Rev.*, 89 (1989) 1875.
12 A. Evers, R.D. Hancock, A.E. Martell, and R.J. Motekaitis, *Inorg. Chem.*, 28 (1989) 2189.
13 A.L. Allred, *J. Inorg. Nucl. Chem.*, 17 (1961) 215.
14 B. Monzyk and A.L. Crumbliss, *Inorg. Chim. Acta*, 55 (1981) L5.
15 B. Monzyk and A.L. Crumbliss, *J. Am. Chem. Soc.*, 104 (1982) 4921.
16 M. Biruš, Z. Bradić, G. Krznarić, N. Kujundžić, M. Pribanić, P.C. Wilkins, and R.G. Wilkins, *Inorg. Chem.*, 26 (1987) 1000.
17 D.J. Lentz, G.H. Henderson, and E.M. Eyring, *Mol. Pharmacol.*, 6 (1973) 514.
18 S.A. Kazmi and S.V. McArdle, *Inorg. Biochem.*, 15 (1981) 153.
19 M. Biruš, Z. Bradić, N. Kujundžić, and M. Pribanić, *Inorg. Chim. Acta*, 56 (1981) L43.
20 M. Biruš, Z. Bradić, N. Kujundžić, and M. Pribanić, *Croat. Chem. Acta*, 56 (1983) 61.
21 M. Biruš, Z. Bradić, N. Kujundžić, and M. Pribanić, *Inorg. Chem.*, 23, (1984) 2170.
22 P. Ackrill, A.J. Ralston, J.P. Day, and K.C. Hooge, *Lancet*, 2 (1980) 692.
23 M. Barry, D.M. Flynn, E.A. Letsky, and R.A. Risdon, *Br. Med. J.*, 2 (1974) 16.
24 D.J. Weatherall, M.J. Pippard, and S.T. Callender, *N. Engl. J. Med.*, 308 (1983) 456.
25 G.D. McLaren, W.A. Muir, and R.W. Kellermeyer, *CRC Crit. Rev. Chem. Lab. Sci.*, 19 (1983) 205.
26 T.P. Tufano and K.N. Raymond, *J. Am. Chem. Soc.*, 103 (1981) 6617.
27 B. Monzyk and A.L. Crumbliss, *J. Inorg. Biochem.*, 19 (1983) 19.
28 G. Schwarzenbach and K. Schwarzenbach, *Helv. Chim. Acta*, 46 (1963) 1390.
29 B. Monzyk and A.L. Crumbliss, *J. Am. Chem. Soc.*, 101 (1979) 6203.
30 M. Biruš, G. Krznarić, N. Kujundžić, and M. Pribanić, *Croat. Chem. Acta*, 61 (1988) 33.
31 B. Monzyk and A.L. Crumbliss, *J. Org. Chem.*, 45 (1980) 4670.
32 B.L. Gould and N. Langermann, *Arc. Biochem. Biophys.*, 215 (1982) 148.
33 C.P. Brink and A.L. Crumbliss, *Inorg. Chem.*, 23 (1984) 4708.
34 A. Dietrich, D.R. Powell, D.L. Eng-Wilmot, M.B. Hossain, and D. van der Helm, *Acta Cryst.*, C46 (1990) 816.
35 A. Dietrich, D.L. Eng-Wilmot, K.A. Fidelis, D.R. Powell, and D. van der Helm, *J. Chem. Soc. Dalton*, submitted for publication.
36 D. van der Helm, M.A.F. Jalal and M.B. Hossain, in G. Winkelmann, D. van der Helm, and J.B. Neilands (Eds.), *Iron Transport in Microbes, Plants and Animals*, VCH Publishers, N.Y., 1987, p. 135.
37 R. Mocharla, D.R. Powell, C.L. Barnes, and D. van der Helm, *Acta Cryst.*, C39 (1983) 868.
38 R. Mocharla, D.R. Powell, and D. van der Helm, *Acta Cryst.*, C40 (1984) 1369.
39 D.R. Powell and D. van der Helm, *Acta Cryst.*, C43 (1987) 493.
40 D. van der Helm, J.R. Baker, R.A. Loghry, and J.D. Ekstrand, *Acta Cryst.*, B37 (1981) 323.
41 D. van der Helm and M. Poling, *J. Am. Chem. Soc.*, 98 (1976) 82.
42 M.B. Hossain, D. van der Helm and M. Poling, *Acta Cryst.*, B39 (1983) 258.
43 W.L. Smith and K.N. Raymond, *J. Am. Chem. Soc.*, 102 (1980) 1252.
44 H.J. Lendner and S. Göttlicher, *Acta Cryst.*, B25 (1969) 832.
45 M. Biruš, Z. Bradić, N. Kujundžić, M. Pribanić, P.C. Wilkins, and R.G. Wilkins, *Inorg. Chem.*, 24 (1985) 3980.

46 L.L. Fish and A.L. Crumbliss, *Inorg. Chem.*, 24 (1985) 2198.
47 M. Biruš, G. Krznarić, M. Pribanić, and S. Uršić, *J. Chem. Res.*(s), 4 (1985).
48 M. Birus, Z. Bradić, N. Kugunžić, and M. Pribanić, *Inorg. Chim. Acta*, 78 (1983) 87.
49 M. Biruš, Z. Bradić, N. Kujundžić, and M. Pribanić, *Acta Pharm. Jugos.*, 32 (1983) 163.
50 T. Emery, *Biochemistry*, 25 (1986) 4629.
51 J.H. Fendler, *Membrane Mimetic Chemistry*, Wiley and Sons, N.Y., 1982.
52 C. Tanford, *The Hydrophobic Effect: Formation of Micelles and Biological Membranes*, Wiley and Sons, N.Y., 1980.
53 R. Ueoka, *Bull. Chem. Soc. Jpn.*, 53 (1980) 347.
54 S.W. Harman, Ph.D. Dissertation, Duke University, 1989.
55 S.W. Harman and A.L. Crumbliss, manuscript in preparation.
56 I.V. Berezin, K. Mortinke, and A.K. Yatsirnirskii, *Rus. Chem. Rev.*, 42 (1973) 787.
57 P. Stilbs, J. Jermer, and B. Lindman, *J. Coll. Interface Sci.*, 60 (1977) 232.
58 S.W. Harman, P.L. Choo and A.L. Crumbliss, manuscript in preparation.
59 D. Stigter and K. Mysels, *J. Phys. Chem.*, 59 (1955) 45.
60 J.T. Davies and E.K. Rideal, *Interfacial Phenomena*, Academic Press, N.Y., 1961, p. 94.
61 C.A. Bunton and B. Wolfe, *J. Am. Chem. Soc.*, 95 (1973) 3742.
62 E. Pelizzetti and E. Pramauro, *Inorg. Chem.*, 19 (1980) 1407.
63 D.J. Ecker, L.D. Loomis, M.E. Cass, and K.N. Raymond, *J. Am. Chem. Soc.*, 110 (1988) 2457.
64 P.L. Choo and A.L. Crumbliss, unpublished results.
65 (a) J.F. Stoddart, in R.M. Izatt and J.J. Christensen (Eds.), *Progress in Macrocyclic Chemistry*, Wiley-Interscience, N.Y., 1981, p. 173; (b) E.P. Kyba, K. Koga, L.R. Sousa, M.G. Siegel and D.J. Cram, *J. Am. Chem. Soc.*, 95 (1973) 2692; (c) D.J. Cram and J.M. Cram, *Science* (Washington, D.C.), 183 (1974) 803.
66 (a) M. Dobler, *Ionophores and Their Structures*, Wiley and Sons, N.Y., 1981, p. 16; (b) H.K. Frensdorff, *J. Am. Chem. Soc.*, 93 (1971) 600.